analytical chemistry

Letter

pubs.acs.org/ac

Electrodeposition of Polydopamine Thin Films for DNA Patterning and Microarrays

Gabriel Loget, Jennifer B. Wood, Kyunghee Cho, Aaron R. Halpern, and Robert M. Corn*

Department of Chemistry, University of California-Irvine, Irvine, California 92697, United States

Supporting Information

ABSTRACT: The controlled electrodeposition of functional polydopamine (PDA) thin films from aqueous dopamine solutions is demonstrated with a combination of electrochemistry, atomic force microscopy (AFM), and surface plasmon resonance (SPR) measurements. PDA micropatterns are then fabricated by electrodeposition on micrometer length scale gold electrodes and used for attaching amino-modified single-stranded DNA (ssDNA). After hybridization with fluorescently labeled ssDNA, the fluorescence microscopy characterization reveals that: (i) PDA can be topographically selectively deposited at the microscale and (ii) electrochemically deposited PDA can be functionalized with amino-terminated ssDNA using the same chemistry as that for spontaneously deposited PDA. Finally, the application of electrodeposited PDA thin films to fabricate ssDNA microarrays is reported using SPR imaging (SPRI) measurements for the detection of DNA and DNA-modified gold nanoparticles.

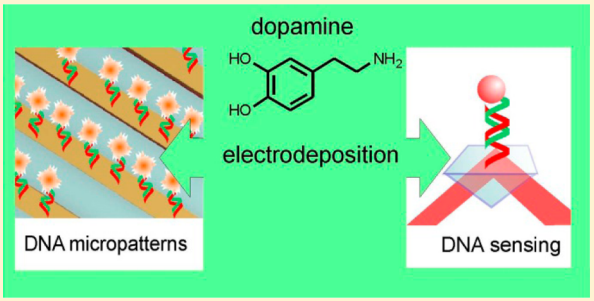

Polydopamine (PDA) is a synthetic eumelanin polymer that exhibits unique biomimetic adhesive properties.[1] Recently, PDA has attracted considerable interest as a thin film coating material[1] on metal, oxide, and biological surfaces and has been applied in optical[2] and electrochemical surface bioaffinity sensing measurements,[3,4] the control of the adhesion of mammalian cells and bacteria to surfaces,[5−8] the fabrication of biomimetic membranes[9] and neural interfaces,[10] and as a thin film substrate for electroless deposition.[5] In the majority of these applications, the polymerization of dopamine is achieved via the chemical process reported by Lee et al.,[5] where a combination of bulk and surface polymerization is induced at a basic pH. While this polymerization strategy is easily implemented, a drawback of this method is that it is difficult to control the spatial localization and surface morphology of the deposited PDA thin film.

An alternative method for the preparation of PDA is through an electrochemical polymerization process. The electrochemical oxidation products of catecholamines are known to polymerize, leading to insulating films on the electrode surface.[11] This phenomenon, often referred to as electrode fouling or poisoning, is usually considered a nuisance in electroanalytical applications but has been shown to be quite effective at electrodepositing homogeneous PDA films. Since the electropolymerization only occurs in the vicinity of the electrode, PDA films can be generated in a highly controlled and spatially selective manner. The mechanism of PDA electropolymerization has been investigated by Li et al.[12] Recently, Tarlov et al. have thoroughly characterized solution polymerized thin films using both electrochemical and spectroscopic methods.[13] A few applications involving electrodeposited PDA films have been reported to date: Łuczak used an overoxidized PDA film for the detection of dopamine;[3] He et al. immobilized immunoglobulin G on electrodeposited PDA;[14] Liu et al. used a molecularly imprinted electrodeposited PDA film for the detection of nicotine;[4] Ouyang et al. reported the enantioselective recognition of glutamic acid using a molecularly imprinted copolymer of electrodeposited PDA and *o*-phenylenediamine,[15] and more recently, Kang et al. used electrodeposited PDA for designing neural interfaces.[10]

Our interest in PDA lies in its applications in the areas of nucleic acid and protein microarrays and biosensors.[16] Specifically, we are interested in high fidelity attachment chemistries for the immobilization of single-stranded DNA (ssDNA) and peptides that have excellent bioavailability for hybridization adsorption of DNA, surface enzyme chemistries of RNA polymerases and ligases, and the specific bioaffinity adsorption of proteins. These chemistries have applications in the areas of DNA microarrays and medical diagnostic devices based on both optical and electrochemical detection methodologies. Chemically deposited[17] PDA films contain catechols and quinones which can covalently bond to amino groups at a slightly basic pH; we have recently used chemically deposited PDA films for the immobilization of amino-terminated ssDNA and for surface plasmon resonance imaging (SPRI) sensing of DNA microarrays.[18] In this context, and due to the actual strong scientific debate concerning the chemical structure of PDA,[17,19] it is of great interest to know if the electrodeposited PDA films can also be used to immobilize nucleic acids.

Received: July 23, 2013
Accepted: October 17, 2013
Published: October 17, 2013

dx.doi.org/10.1021/ac4022743 | *Anal. Chem.* 2013, 85, 9991−9995

In this paper, we first characterize the PDA electrodeposited thin films with a combination of electrochemistry, atomic force microscopy (AFM), and surface plasmon resonance (SPR) measurements. In a second set of experiments, we fabricate micrometer-scale patterns of electrodeposited PDA and use them for attaching amino-modified ssDNA. After the hybridization of complementary DNA, these thin films are characterized with fluorescence microscopy. Finally, we demonstrate the utility of electrodeposited PDA thin films for the fabrication of ssDNA microarrays, that are used for monitoring the bioaffinity adsorption of DNA and DNA-modified gold nanoparticles microarrays with SPRI.

RESULTS AND DISCUSSION

Electrodeposition of PDA Thin Films at the Macroscale: Electrochemical and SPR Characterization. The electrodeposition of PDA thin films from aqueous dopamine solutions was characterized with a combination of cyclic voltammetry (CV) and in situ scanning angle SPR measurements on macroscale (1.5 cm^2) gold thin film (45 nm) working electrodes. The experimental cell is described in the Supporting Information (Figure S1). The gold electrode was exposed to a 5 mM dopamine solution buffered to a pH of 6.5. At this pH, no spontaneous polymerization of dopamine to PDA either in solution or on the gold surface was observed. A series of up to 60 CV scans were recorded and are shown in Figure 1a.

Figure 1b shows the 20th CV scan; four redox peaks are present in the CV. The first anodic peak, a1, at 0.46 V is attributed to the oxidation of dopamine leading to dopaminequinone. Dopaminequinone undergoes several chemical (denoted by "C") and electrochemical (denoted by "E") transformations, which leads to PDA. An "ECECEE" mechanism was proposed by Li et al. involving 5,6-indolequinone as the polymerizable species.[12] According to this group, the two cathodic peaks c1 and c2 at −0.02 and −0.34 V may be attributed to the reductions of dopaminequinone and dopaminechrome, respectively. The second anodic peak, a2, at −0.16 V may be attributed to the oxidation of leucodopaminechrome (the reduction product of dopaminechrome).[12] During the first 50 scans, the continuous drop in electrode activity due to the formation of PDA passivating multilayer is revealed by the decrease of the anodic and cathodic currents during the process. This important feature demonstrates the fouling of the electrode by the PDA layer as it grows with each successive scan. From the 50th scan, a steady state voltammogram is obtained, which is plotted in Figure 1c, where no more electron transfer between the gold surface and the species in solution is allowed due to the total fouling of the electrode by the PDA. Two redox peaks are still present after the 50th scan at 0.22 and 0.13 V, which we attribute to the oxidation and reduction of the catechols and quinones units present in the PDA, close enough to the gold surface to undergo electron transfer. A key result is that, after 50 scans, there is complete blocking of solution electrochemistry, indicating the formation of a contiguous PDA film. These results are consistent with the recent measurements on the characterization of PDA films by Tarlov et al.[13]

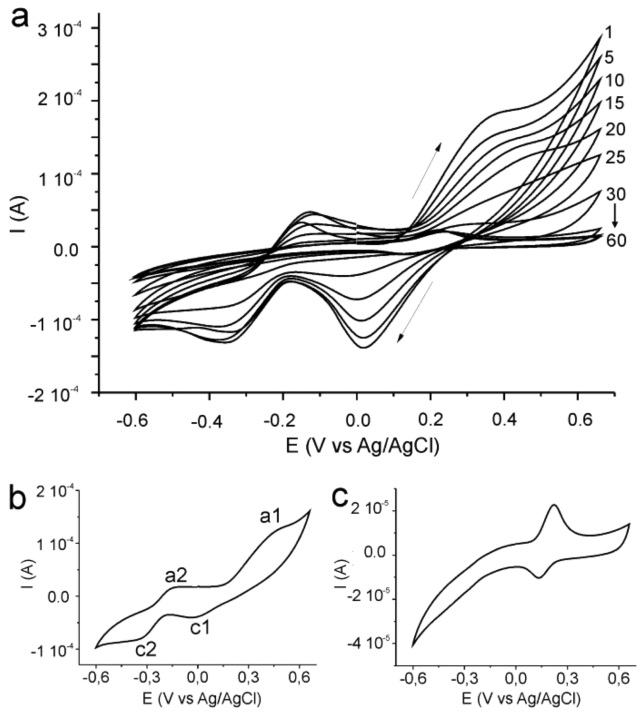

Figure 1. PDA film growth by cyclic voltammetry. (a) Cyclic voltammograms of a solution of 5 mM dopamine, on gold, in phosphate buffer (pH 6.5) with a scan rate of 20 mV s^{-1}. The 1st, 5th, 10th, 15th, 20th, 25th, 30th, 40th, 50th, and 60th scans are shown; the arrows indicate the sweep direction. (b) 20th scan. (c) 50th scan.

Along with the voltammograms, an SPR scanning angle curve (percent reflectivity at 814 nm vs incident angle) was obtained after each CV scan. Figure 2a shows the in situ scanning angle reflectivity curves recorded directly after the CV scans, from the bare gold surface (curve 0) to the 30th scan. The SPR angle θ_{spr} equals 53.555° for the initial bare gold surface and shifts toward higher angles for each successive scan reaching 54.574° after 30 scans. This shift, proportional to the thickness of the polymer layer, confirms the deposition of the PDA film onto the gold surface. The SPR angle shift as a function of the number of scans, plotted in Figure 2b, was found to be linear after 10 scans at a rate of 0.042° $scan^{-1}$. The sublinear regime observed before 10 scans is attributed to the initial generation and growth of PDA nuclei on the gold electrode surface before homogeneous film growth initiates at 10 scans.

In addition to the in situ SPR scanning angle measurements, a set of ex situ SPR and AFM measurements were obtained for three dried PDA films electrodeposited with 5, 20, and 30 CV scans. Table 1 lists the results of these measurements. The AFM measurements vary linearly with CV number, from 0.91 nm for the thinnest film to 5.14 nm for the thickest film. This data shows that the PDA thickness can be easily tuned by controlling the number of scans. The roughness of the PDA films was also found to increase with the scan number; a maximum roughness of ±0.36 nm was obtained for the film deposited with 30 CV scans (Table 1). The three dried films were also characterized by ex situ SPR measurements. Using the AFM thicknesses, a five-phase Fresnel calculation was used to fit the SPR data obtained for 20 and 30 CV scans. The fits are shown in Figure S2 in the Supporting Information. From these values, we report an average refractive index of $n = 1.55 \pm 0.05$ with an imaginary part $k = 0.04$ for these PDA thin films at a wavelength of 633 nm. This n value is in the range of refractive index documented for organic polymers.[20]

Micropatterned Electrodeposited PDA Thin Films and Fluorescence Measurements of DNA Hybridization Adsorption. Here, we demonstrate the toposelective electrodeposition of PDA at the microscale, as well as the possibility to

dx.doi.org/10.1021/ac4022743 | Anal. Chem. 2013, 85, 9991−9995

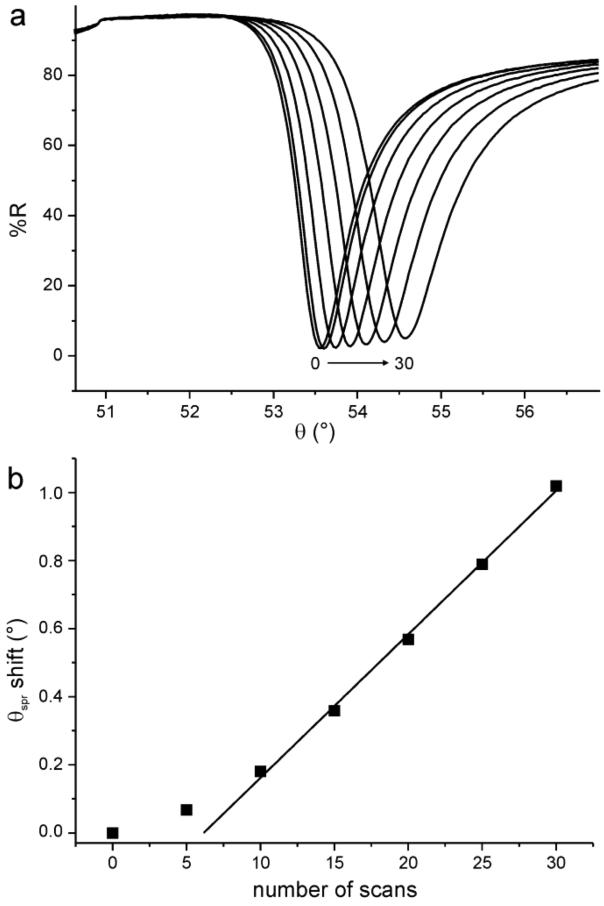

Figure 2. In situ scanning angle SPR measurement of PDA film growth. (a) Scanning angle SPR curves (reflectivity at 814 nm vs incident angle) corresponding to the bare gold surface (curve 0) and the 5th, 10th, 15th, 20th, 25th, and 30th scans during the CV shown in Figure 1. (b) Plot of the shift in SPR angle as a function of CV scan.

Table 1. Ex Situ Characterization of Electrodeposited PDA Thin Films[a]

	number of CV scans	t (nm)	θ_{spr} (°)
1	5	0.91 ± 0.12	43.526
2	20	2.48 ± 0.21	43.836
3	30	5.14 ± 0.36	44.279

[a]Values of film thickness, t, obtained by AFM measurements and the SPR angle θ_{spr}.

functionalize electrodeposited PDA with amino-terminated ssDNA using the chemical procedure reported recently for spontaneously deposited PDA.[18] The demonstration of the latter point was driven by the actual controversy on the chemical structure of PDA,[17,19] which means that it is not straightforward that electrochemically deposited PDA can be functionalized by amino-terminated ssDNA as it is the case for spontaneously deposited PDA. Spontaneously deposited PDA thin films contain catechols and quinones moieties[17] that can generate covalent bonds at slightly basic pHs with molecules possessing amino groups via Schiff base or Michael addition reactions.[1,5] The modification of chemically deposited PDA thin films with molecules containing amino groups has been reported previously.[5,18] The first example for electrodeposited PDA is reported in Figure 3a. First, the PDA electrodeposition (20 scans) was performed on gold stripes having a width of 4

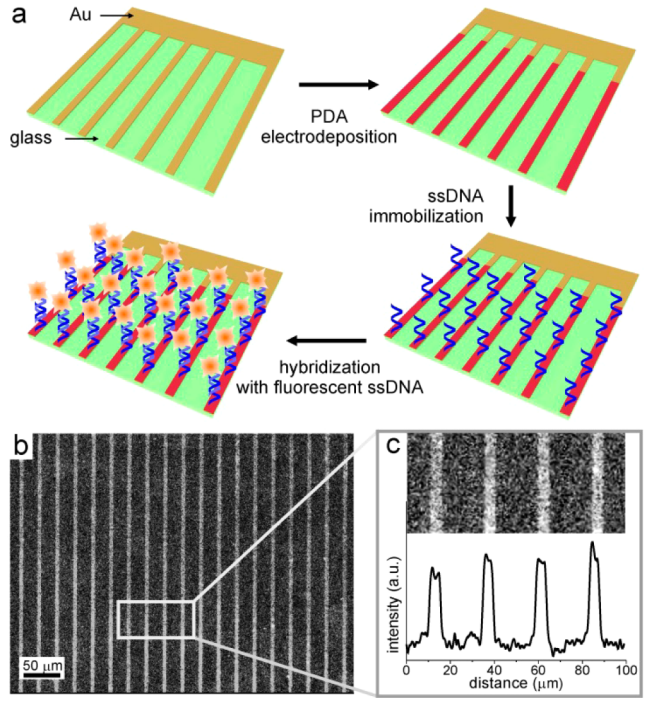

Figure 3. Hybridization of fluorescent DNA on electrodeposited PDA micropatterns. (a) Schematic of the steps used for the fluorescence hybrization experiment. First, PDA was electrodeposited on the gold microelectrode array. The PDA was then modified with an amino-terminated ssDNA, and finally, the fluorophore-labeled ssDNA was exposed on the PDA array. (b) Fluorescent micrograph obtained after the hybridization of the fluorescent ssDNA on the PDA microstripes previously modified with the complementary ssDNA. (c) Magnification of the section squared in (b) and the corresponding intensity profile.

μm and spaced by 21 μm. The electrodeposited PDA thin films were functionalized with ssDNA using the same procedure as for the previous SPRI experiments reported for spontaneously deposited PDA.[18] Basically, a slightly basic (Tris buffer, pH 8.5) solution containing the amino-terminated ssDNA (1 mM) was spotted on the gold/PDA micropatterned array and left overnight for the covalent attachment to proceed. For the hybridization, the gold/PDA arrays were exposed to complementary ssDNA labeled with a fluorophore (Cy3) and the array was observed under a fluorescence microscope. Figure 3b shows a fluorescence image of the microelectrode array after the hybridization. The gold/PDA stripes are clearly revealed since the width of the fluorescence stripes, 4.2 μm, as determined by the half peak width on the intensity profile of Figure 3c, corresponds to the width of the patterned gold stripes. A control experiment, where a noncomplementary amino-terminated ssDNA was immobilized, was performed and did not exhibit any measurable fluorescence after exposure to the Cy3-labeled ssDNA. These experiments prove: (i) that PDA thin films can be deposited locally on the micrometer length scale by this electrochemical method and (ii) that electrodeposited PDA can be readily functionalized with amino-terminated ssDNA using the straightforward protocol reported for spontaneaously deposited PDA.[18] The use of electrochemistry for depositing toposelectively PDA is strongly advantageous over depositing dopamine chemically because, in the latter case, the deposition occurs from a combination of

dx.doi.org/10.1021/ac4022743 | Anal. Chem. 2013, 85, 9991−9995

surface and bulk phase polymerization processes, which cannot lead to a toposelective deposition.

SPRI Measurements of DNA Microarrays Fabricated on Electrodeposited PDA Thin Films. Having demonstrated and characterized the electrodeposited PDA thin films and shown that amino-terminated ssDNA can be attached to them, we finally show the application of such coatings for the fabrication of ssDNA microarrays. As first proof-of-principle examples, we have immobilized amino-functionalized ssDNA on the electrodeposited PDA patterns and used these surfaces to detect DNA by hybridization adsorption.

As shown in Figure 4, prior to SPRI, gold stripes having a width of 1 mm and connected together with a contact pad were

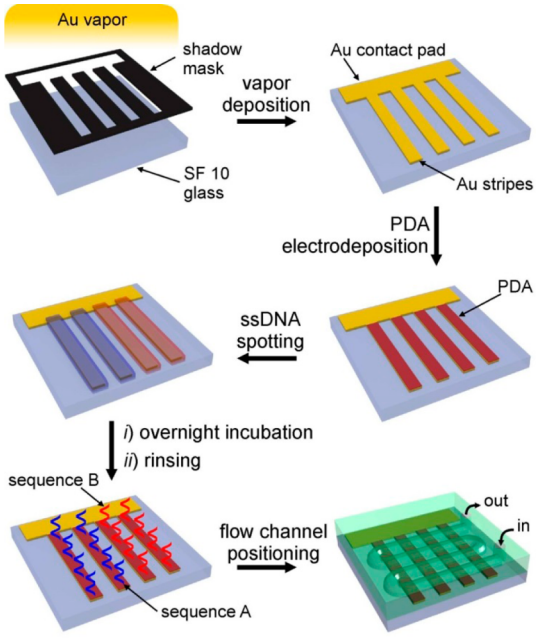

Figure 4. Schematic showing the fabrication of the DNA microarray used for SPRI experiments.

fabricated by thermal deposition with a shadow mask on a SF10 glass slide. PDA was first electrodeposited on the gold thin film strips (patterned on SF10 glass) by running 20 CV scans. The gold stripes were then exposed to two different amino-terminated ssDNA in Tris buffer (pH 8.5) and left overnight for the DNA to bind with the PDA. The bioavailability of the ssDNA attached to the electrodeposited PDA thin film was measured by SPRI measurements of the hybridization adsorption of complementary DNA and DNA-modified gold nanoparticles. The optical technique of SPRI is a highly effective method for detecting bioaffinity adsorption onto the DNA microarray via changes in the local refractive index.[21,22] The DNA-modified gold thin film stripes were rinsed and used for SPRI with a microfluidic flow cell that is similar to the one employed in previous SPRI measurements.[23,24] For the SPRI experiment shown in Figure 5a, 13 nm gold nanoparticles (AuNPs) modified with ssDNA complementary to only one of the immobilized ssDNA were used in order to enhance the SPRI signal.[23,25] The AuNPs were injected into the flow cell, and Figure 5b shows the real-time quantitative plots of reflectivity change ($\Delta\%R$) on the gold/PDA stripes modified with the complementary ssDNA (blue curve) and the noncomplementary ssDNA (red curve). The successful hybrid-

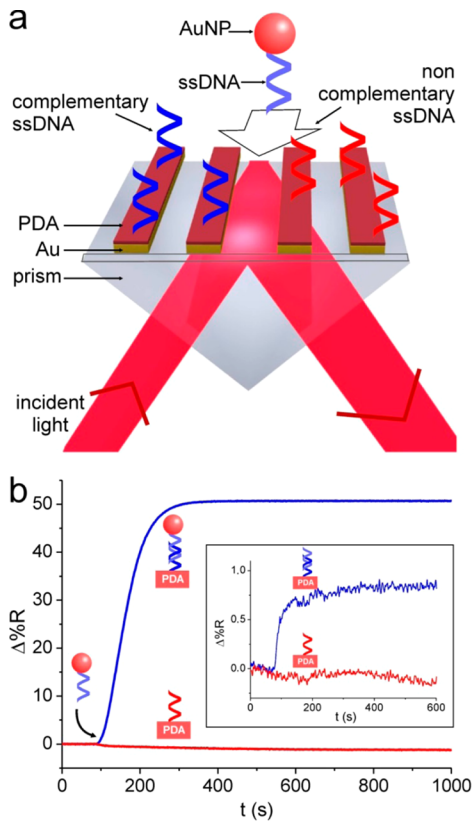

Figure 5. In situ detection of DNA hybridization on electrodeposited PDA. (a) Schematic showing the SPRI experiment. (b) Quantitative plots of SPRI reflectivity change as a function of time after the exposure of complementary ssDNA-modified PDA (blue curve) and noncomplementary ssDNA-modified PDA (red curve) to AuNPs labeled with ssDNA. Inset: Quantitative plot of SPRI reflectivity change after the exposition of ssDNA-modified PDA (blue curve) and noncomplementary ssDNA-modified PDA (red curve) to a random sequence ssDNA.

ization with complementary target DNA generated a significant increase in the reflectivity of more than 50 $\Delta\%R$ (50.68 ± 0.08) after 311 s, whereas the exposure with noncomplementary DNA did not significantly affect the reflectivity. This maximum reflectivity shift is in good agreement with the value expected for a full monolayer of AuNPs previously reported using poly-L-glutamic acid as the attachment layer.[23] Such a high increase in values of reflectivity in the first case is due to the enhancement by the AuNP labeled complementary DNA.[23,25] In this experiment, the use of electrodeposited PDA provides a distinct and nearly ideal detection of complementary DNA without any false-positive signal increase for noncomplementary as the negative control. As shown in the inset of Figure 5b, the hybridization of a random sequence ssDNA can also be detected without the use of AuNPs but with a considerably smaller reflectivity change than that obtained with the AuNP-labeled ssDNA. These SPRI data further demonstrate that electrodeposited PDA films can be functionalized with ssDNA and that those films can be used for the fabrication of DNA microarrays.

CONCLUSIONS

In this paper, we have demonstrated the controlled electrochemical deposition of PDA onto gold surfaces. The electropolymerization process was characterized with a combination of

dx.doi.org/10.1021/ac4022743 | Anal. Chem. 2013, 85, 9991−9995

cyclic voltammetry, in situ and ex situ SPR angle shift measurements and AFM film thickness measurements. Compared to solution deposition methods of PDA thin film formation, the great advantage of the electrodeposition method is that it allows the formation of PDA patterns and arrays with toposelective control. We further demonstrated the one-step immobilization of ssDNA onto micropatterned thin films and characterized them by fluorescence microscopy. Finally, we showed the utility of such electrodeposited structures for fabricating DNA microarrays that we used for nucleic acid bioaffinity sensing using SPRI. Electrochemically PDA-functionalized arrays of metal or semiconductor elements on the micrometer length scale could be very useful in the fabrication DNA microchips. Additionally, the sequential modification of interdigitated microelectrode arrays with ssDNA for electrochemical DNA sensors is easily implemented with this electrodeposition method as compared to the fastidious spotting of dopamine solutions that would be required with the alternative spontaneous solution polymerization process.

■ ASSOCIATED CONTENT

Supporting Information

The experimental procedures and the fitting of the SPR curves. This material is available free of charge via the Internet at http://pubs.acs.org.

■ AUTHOR INFORMATION

Corresponding Author

*E-mail: rcorn@uci.edu.

Author Contributions

The manuscript was written through contributions of all authors. All authors have given approval to the final version of the manuscript.

Notes

The authors declare no competing financial interest.

■ ACKNOWLEDGMENTS

This work was supported by the NSF through grant CHE-1057638. The authors thank Prof. R. M. Penner for the use of his AFM.

■ REFERENCES

(1) Lynge, M. E.; van der Westen, R.; Postma, A.; Stadler, B. *Nanoscale* **2011**, *3*, 4916−4928.
(2) Morris, T. A.; Peterson, A. W.; Tarlov, M. J. *Anal. Chem.* **2009**, *81*, 5413−5420.
(3) Łuczak, T. *Electrochim. Acta* **2008**, *53*, 5725−5731.
(4) Liu, K.; Wei, W.-Z.; Zeng, J.-X.; Liu, X.-Y.; Gao, Y.-P. *Anal. Bioanal. Chem.* **2006**, *385*, 724−729.
(5) Lee, H.; Dellatore, S. M.; Miller, W. M.; Messersmith, P. B. *Science* **2007**, *318*, 426−430.
(6) Lai, M.; Cai, K.; Zhao, L.; Chen, X.; Hou, Y.; Yang, Z. *Biomacromolecules* **2011**, *12*, 1097−1105.
(7) Liu, A.; Zhao, L.; Bai, H.; Zhao, H.; Xing, X.; Shi, G. *ACS Appl. Mater. Interfaces* **2009**, *1*, 951−955.
(8) Kang, S.; Elimelech, M. *Langmuir* **2009**, *25*, 9656−9659.
(9) McCloskey, B. D.; Park, H. B.; Ju, H.; Rowe, B. W.; Miller, D. J.; Chun, B. J.; Kin, K.; Freeman, B. D. *Polymer* **2010**, *51*, 3472−3485.
(10) Kang, K.; Lee, S.; Kim, R.; Choi, I. S.; Nam, Y. *Angew. Chem., Int. Ed.* **2012**, *51*, 13101−13104.
(11) Lane, R. F.; Hubbard, A. T. *Anal. Chem.* **1976**, *48*, 1287−1293.
(12) Li, Y.; Liu, M.; Xiang, C.; Xie, Q.; Yao, S. *Thin Solid Films* **2006**, *497*, 270−278.
(13) Zangmeister, R. A.; Morris, T. A.; Tarlov, M. J. *Langmuir* **2013**, *29*, 8619−8628.
(14) He, H.; Xie, Q.; Yao, S. *J. Colloid Interface Sci.* **2005**, *289*, 446−454.
(15) Ouyang, R.; Lei, J.; Ju, H.; Xue, Y. *Adv. Funct. Mater.* **2007**, *17*, 3223−3230.
(16) Sassolas, A.; Leca-Bouvier, B. D.; Blum, L. J. *Chem. Rev.* **2007**, *108*, 109−139.
(17) Dreyer, D. R.; Miller, D. J.; Freeman, B. D.; Paul, D. R.; Bielawski, C. W. *Langmuir* **2012**, *28*, 6428−6435.
(18) Wood, J. B.; Szyndler, M. W.; Halpern, A. R.; Cho, K.; Corn, R. M. *Langmuir* **2013**, *29*, 10868−10873.
(19) Liebscher, J.; Mrówczyński, R.; Scheidt, H. A.; Filip, C.; Hădade, N. D.; Turcu, R.; Bende, A.; Beck, S. *Langmuir* **2013**, *29*, 10539−10548.
(20) Katritzky, A. R.; Sild, S.; Karelson, M. *J. Chem. Inf. Model.* **1998**, *38*, 1171−1176.
(21) Thiel, A. J.; Frutos, A. G.; Jordan, C. E.; Corn, R. M.; Smith, L. M. *Anal. Chem.* **1997**, *69*, 4948−4956.
(22) Brockman, J. M.; Frutos, A. G.; Corn, R. M. *J. Am. Chem. Soc.* **1999**, *121*, 8044−8051.
(23) Sendroiu, I. E.; Gifford, L. K.; Lupták, A.; Corn, R. M. *J. Am. Chem. Soc.* **2011**, *133*, 4271−4273.
(24) Wegner, G. J.; Lee, H. J.; Marriott, G.; Corn, R. M. *Anal. Chem.* **2003**, *75*, 4740−4746.
(25) Fang, S.; Lee, H. J.; Wark, A. W.; Corn, R. M. *J. Am. Chem. Soc.* **2006**, *128*, 14044−14046.